

Phase diagram of the ABC model with nonequal densities

O Cohen and D Mukamel

Department of Physics of Complex Systems, Weizmann Institute of Science, Rehovot 76100, Israel

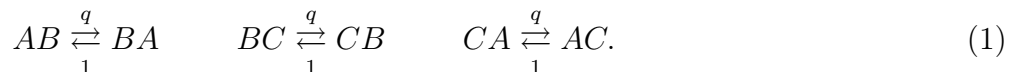
E-mail: or.cohen@weizmann.ac.il and david.mukamel@weizmann.ac.il

Abstract. The ABC model is a driven diffusive exclusion model, composed of three species of particles that hop on a ring with local asymmetric rates. In the weak asymmetry limit, where the asymmetry vanishes with the length of the system, the model exhibits a phase transition between a homogenous state and a phase separated state. We derive the exact solution for the density profiles of the three species in the hydrodynamic limit for arbitrary average densities. The solution yields the complete phase diagram of the model and allows the study of the nature of the first order phase transition found for average densities that deviate significantly from the equal densities point.

PACS numbers: 05.50.+q, 05.70.Ln and 64.60.Cn

1. Introduction

Systems that are driven out of equilibrium by an external field, such as temperature gradient or electric field, have been studied extensively in recent years. In the absence of a general theory, insight into their properties can be acquired by investigating simplified models. Studies of numerous driven models involving some conserved quantity have shown that their steady state typically exhibits algebraic decay of correlations [1–5] and in some cases long-range order and symmetry breaking in one dimension [6–10]. One particular model which has drawn much attention recently is the ABC model [9, 10]. This is a prototypical model for phase separation in one dimension. It consists of a periodic lattice of length L where each site is occupied by one of the three species of particles, labeled A , B and C . The model evolves by random sequential updates whereby particles on nearest neighbour sites are exchanged with rates



While for $q = 1$ the model relaxes to an equilibrium state with homogeneously distributed particles, it exhibits phase separation for any finite value of $q \neq 1$ in the limit of $L \rightarrow \infty$. Generically, for arbitrary choice of the number of particles of the three species, N_A, N_B and N_C , the model does not obey detailed balance and it relaxes to a nonequilibrium steady-state. A unique feature of the ABC model is that in the special case of $N_A = N_B = N_C$ the dynamics obeys detailed balance with respect to an effective Hamiltonian with *long-range interactions* for arbitrary value of q . This Hamiltonian provides a rare opportunity to gain insight into the mechanism behind phase separation in one dimension induced by a drive in the bulk.

The ABC model has been considered in the weak asymmetry limit where q approaches 1 in the thermodynamic limit as $q = \exp(-\beta/L)$ [11]. When the rate of approach is faster than a critical value, namely for $\beta < \beta_c$, the model reaches a homogenous phase in the limit of $L \rightarrow \infty$. For $\beta > \beta_c$ the model reaches an ordered phase with three macroscopic domains, each predominantly occupied by one of the species. The phase transition has been studied in the hydrodynamic limit by analyzing the linear response of the homogenous phase to small inhomogeneous perturbations. In the equal densities case, the transition was found to be continuous, taking place at $\beta = \beta_c = 2\pi\sqrt{3}$. The transition remains continuous for small enough deviation from the equal-densities condition, and becomes first order beyond a tricritical point at larger deviations. Since the analysis was based on linear stability of the homogenous phase, the full phase diagram of the model and the nature of the first order transition could not be explored. This would require the knowledge of the density profiles of the three species in the ordered phase.

In the present paper we derive an exact expression for the steady-state density profiles of the ABC model for arbitrary values of average densities and β by solving the hydrodynamic equations corresponding to the evolution of the model. We use our results to investigate its phase diagram and the nature of the first order phase transition.

Beyond the tricritical point we find a range of temperatures where both the homogeneous and ordered phases are locally stable. The phase to which the model eventually relaxes could in principle be determined by minimizing the large deviation function. Since this function is known only in the limit of weak drive ($\beta \ll 1$) [11] and for small deviations from the homogeneous phase [12], we can only draw the stability limits of each phase. These limits define the region of parameter space where both phases are locally stable.

The ABC model has recently been generalized to include particle-nonconserving processes and its phase diagram has been analyzed in the equal densities case [13, 14]. The phase diagrams of the canonical (particle-conserving) and grand canonical (particle-nonconserving) ensembles have been shown to be inequivalent. This is in accordance with what is generally expected in equilibrium systems with long-range interactions. The study presented in this paper of the nature of the phase-separated state can be generalized to the case of the nonconserving ABC model with arbitrary densities. This would enable one to explore phenomena such as inequivalence of ensembles in a genuinely driven model which does not obey detailed balance [15].

The paper is organized as follows. We first present a brief review of the ABC model and previous studies of its phase diagram in section 2. We derive the steady-state of the hydrodynamic equations of the model in section 3, and express it explicitly in terms of elliptic integrals in Appendix A. In section 4 we study the resulting phase diagram of the model and compare it with results from Monte Carlo simulations. The low temperature (strong drive) behaviour of the solution is derived in Appendix B.

2. Phase diagram derived from stability analysis

In this section we present the ABC model and review its properties and phase diagram, obtained in previous studies using stability analysis of the homogeneous phase.

In studying the ordered phase of the ABC model one notes that for $q < 1$ the ordered phase is such that the domains are arranged clockwise as $AA \dots ABB \dots BCC \dots C$, and counterclockwise for $q > 1$. Throughout this paper we consider $q < 1$. The case of $q > 1$ is obtained by permutating for instance the labels of the B and C in a system where the drive is given by $q' = 1/q < 1$.

As a result of the dynamical asymmetry, the model generically reaches a nonequilibrium steady state with nonvanishing currents of particles. The current of, say, the A particles is proportional to the rate at which they perform a full clockwise trip minus the rate of the counter-clockwise trip, yielding

$$J_A \sim q^{N_B} - q^{N_C}. \quad (2)$$

The other currents are obtained by cyclic permutation of the A, B and C labels. While these currents vanish in the thermodynamic limit for arbitrary average densities, in the special case where $N_A = N_B = N_C = L/3$, the currents also vanish for finite systems with arbitrary length. In this case the dynamics obeys detailed balance with respect to

an effective long-range Hamiltonian given by

$$\mathcal{H}(\zeta) = \sum_{i=1}^L \sum_{k=1}^{L-1} \frac{k}{L} (A_i B_{i+k} + B_i C_{i+k} + C_i A_{i+k}), \quad (3)$$

where $\zeta = \{\zeta_i\}_{i=1}^L$ denotes a microstate of the system such that $\zeta_i = A, B$ or C . The operators in the Hamiltonian are defined as

$$A_i = \begin{cases} 1 & \zeta_i = A \\ 0 & \text{else} \end{cases}. \quad (4)$$

and similarly for B_i and C_i . The probability of a microscopic configuration is given by $P(\zeta) \propto q^{\mathcal{H}(\zeta)}$. The Hamiltonian yields a super-extensive energy which scales as $E \sim L^2$ with the system size, typical of systems with long-range interactions.

As mentioned in the introduction, the ABC model is often considered in the limit of weak asymmetry, $q = \exp(-\beta/L)$, where β is regarded as the inverse temperature of the model [11]. This rescaling of the drive with L corresponds to the Kac prescription for the rescaling of the temperature in long-range interacting systems [16]. It amounts to an effective rescaling of the energy so it becomes linear with the system size, thus comparable to the entropy, $S \sim L$. Study of this limit for the equal densities case revealed a second order phase transition at $\beta = 2\pi\sqrt{3}$ from the homogeneous state, where entropy dominates, to the ordered state which is dominated by the energy term.

The ABC model has also been studied on an interval, where zero flux boundary condition is considered [17–19]. In that case the model obeys detailed balance also for nonequal densities and its steady state can be obtained using the same effective Hamiltonian (3). The steady-state density profiles of the three species in the phase separated state of this model has been evaluated for arbitrary values of average densities [17]. In the special case of equal densities, the steady state of the model on an interval and that on a ring are related by a trivial mapping, allowing us to use the studies of the model on the interval as a point of reference for the present work.

In the case of equal densities on a ring or arbitrary densities on an interval, where an effective Hamiltonian can be defined, it has been demonstrated that due to the weak anisotropy limit local density correlations vanish for $L \rightarrow \infty$. Namely,

$$\langle X_i Y_{i+1} \rangle = \langle X_i \rangle \langle Y_{i+1} \rangle + O(1/L). \quad (5)$$

where X, Y denote either A, B or C and $\langle \ \rangle$ denotes an ensemble averages over the steady-state distribution. It has been argued that this lack of local correlation is valid also for nonequal densities on a ring [17]. As a result of (5) the hydrodynamic equations [17, 20, 21] corresponding to this model are given by

$$\frac{\partial \rho_\alpha}{\partial \tau} = \beta \frac{\partial}{\partial x} [\rho_\alpha (\rho_{\alpha+1} - \rho_{\alpha+2})] + \frac{\partial^2 \rho_\alpha}{\partial x^2}, \quad (6)$$

where τ is the macroscopic time-scale and $\rho_\alpha(x)$ is the coarsed-grained density profile of particles of type α for $x \in [0, 1]$. The index α denotes the species and runs cyclicly over A, B and C . The conservation of particles implies that $\int_0^1 dx \rho_\alpha(x) = N_\alpha/L \equiv r_\alpha$,

where r_α is the average density of particle α . Since $r_A + r_B + r_C = 1$ it is convenient to express the densities in terms of two independent variables as

$$(r_A, r_B, r_C) = \left(\frac{1}{3}, \frac{1}{3}, \frac{1}{3}\right) + 2\Delta \left(\sin \phi, \sin \left(\phi + \frac{2\pi}{3}\right), \sin \left(\phi + \frac{4\pi}{3}\right)\right), \quad (7)$$

where $\Delta^2 = \frac{1}{6} \sum_{\alpha=A,B,C} (r_\alpha - \frac{1}{3})^2$ is a measure for the deviation from equal densities and ϕ is a phase variable.

It is easy to see that the homogenous profile, $\rho_\alpha(x) = r_\alpha$, is a solution of (6). Its stability with respect to small anisotropic perturbations revealed a critical line given by

$$\beta = \frac{2\pi\sqrt{3}}{\sqrt{1 - 36\Delta^2}}. \quad (8)$$

The homogenous phase was found to be unstable at temperatures ($T = 1/\beta$) below this line [11]. Probing the region just below the critical line, infinitesimal perturbations around the homogenous phase were found to be stable only when r_α obey

$$S(r_A, r_B, r_C) = (r_A^2 + r_B^2 + r_C^2) - 2(r_A^3 + r_B^3 + r_C^3) < 0. \quad (9)$$

For these values the model undergoes a continuous second order transition at (8), whereas for other values of r_α the transition becomes first order. The tricritical line, where the order of the transition changes, is given by $S(r_A, r_B, 1 - r_A - r_B) = 0$ and in terms of Δ, ϕ by

$$108 \sin(3\phi) \Delta^3 - 54\Delta^2 + 1 = 0. \quad (10)$$

The resulting phase diagram is shown in figure 1 for the case of two nonequal densities, defined by taking $\phi = 7\pi/6$ as

$$r_A = r_B = 1/3 - \Delta, \quad r_C = 1/3 + 2\Delta. \quad (11)$$

The critical line and tricritical point in the figure are based on the work of Clincy et al., while the upper stability line is drawn based on the results presented in the two following sections. Note that the phase diagram is not symmetric around $\Delta = 0$. At one end of the phase diagram, for $\Delta = 1/3$, we obtain $r_C = 1$ and hence no dynamics, whereas for $\Delta = -1/6$ we obtain the weakly asymmetric exclusion process with $r_A = r_B = 1/2$ [1].

While the critical line and the tricritical point can be found by expanding (6) near the homogenous solution, studying the first order transition and the stability limit of the phase separated state requires the knowledge of exact density profiles. In this paper we calculate the steady-state density profiles of the model and use them to analyze its complete phase diagram. An exact solution of (6) on an interval has been derived by Ayyer et al. [17]. Following a similar derivation, we generalize their solution to the nonequal-densities regime of the periodic model. This allows us to study the nature of the first order transition phase predicted by Clincy et al.

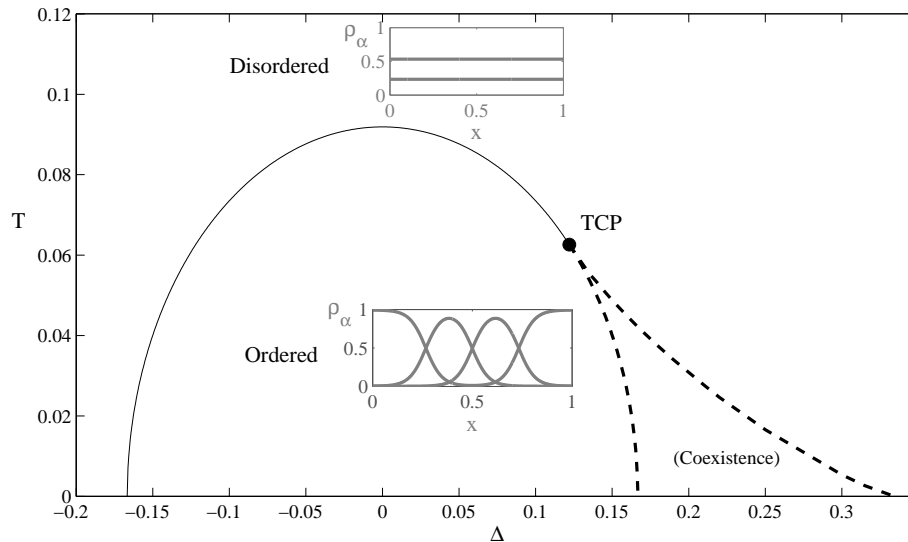


Figure 1. ($T \equiv 1/\beta, \Delta$) phase diagram of the ABC model for two nonequal densities. The solid line denotes the second order phase transition which turns into first order at the tricritical point (TCP). The first order transition is depicted by two stability line (dashed lines) where the two phases coexist.

3. Density profiles for nonequal densities

In this section we study the steady-state solutions of the hydrodynamic equations of the ABC model (6). Assuming time-independent solutions, we omit the time derivative from (6) and integrate over x to yield

$$\frac{\partial \rho_\alpha}{\partial x} = -\beta [\rho_\alpha (\rho_{\alpha+1} - \rho_{\alpha+2})] - J_\alpha, \quad (12)$$

where the constants of integration, J_α , are interpreted as the steady-state currents of particles. They can be shown to obey $J_A + J_B + J_C = 0$. In order to solve (12) we apply several transformations which are similar to those used by Ayyer et al. for the ABC model on an interval [17]. Multiplying (12) by $\rho_{\alpha+1}\rho_{\alpha+2}$ and summing the three resulting equations yields

$$\begin{aligned} \frac{\partial}{\partial x} (\rho_A \rho_B \rho_C) &= -J_A \rho_B \rho_C - J_B \rho_C \rho_A - J_C \rho_A \rho_B \\ &= -\frac{J_A}{\beta} \frac{\partial \rho_C}{\partial x} + \frac{J_C}{\beta} \frac{\partial \rho_A}{\partial x}. \end{aligned} \quad (13)$$

Integrating this equation over x yields a simple relation between the density profiles,

$$\rho_A \rho_B \rho_C = K - Q_A \rho_C + Q_C \rho_A, \quad (14)$$

where $Q_\alpha \equiv J_\alpha/\beta$ and K is a constant of integration. One can check that this equation is indeed invariant under cyclic permutations of A, B and C up to a change in the constant of integration, K . Equation (14) is a generalization of the relation obtained for the equal densities case, where $\rho_A(x)\rho_B(x)\rho_C(x)$ has been shown to be constant in

space [17, 21]. Using (14) in conjunction with $\rho_B = 1 - \rho_A - \rho_C$ allows us to express ρ_A in terms of ρ_C as

$$\rho_A = \frac{-(\rho_C^2 - \rho_C + Q_C) \pm \sqrt{(\rho_C^2 - \rho_C + Q_C)^2 + 4Q_A\rho_C^2 - 4K\rho_C}}{2\rho_C} \quad (15)$$

Inserting this expression back in (12) for $\alpha = C$ yields an explicit equation for ρ_C ,

$$\frac{\partial \rho_C}{\partial x} = \pm \sqrt{(\rho_C^2 - \rho_C + Q_C)^2 + 4Q_A\rho_C^2 - 4K\rho_C}. \quad (16)$$

The plus and minus signs correspond to the two halves of the ring around the maximum of $\rho_C(x)$. Taking the square of this equation and writing it in the rescaled variables $t = 2\beta x$ and $y(t) = \rho_C(x)$ we obtain

$$\frac{1}{2}y'(t)^2 + U_{K,Q_A,Q_C}(y(t)) = 0, \quad (17)$$

where

$$U_{K,Q_A,Q_C}(y) = -\frac{1}{8}y^2(1-y)^2 + \frac{2K + Q_C}{4}y - \frac{2Q_A + Q_C}{4}y^2 - \frac{Q_C^2}{8}. \quad (18)$$

Equation (17) can be viewed as an equation of motion of a zero-energy particle with mass 1 in a quartic potential. Equation (17) and the derivation below can be written in terms of either of the three species by cyclic permutation of A, B and C . In the nonequal densities case the quartic potential changes under this permutation, yielding a different profile for each species.

Depending on the values of K, Q_A and Q_C the potential may have two, three or four real roots, depicted in the (i),(ii) and (iii) lines in figure 2, respectively. The four roots of the potential, denoted as $\{a, b, c, d\}$ can be shown to obey $0 \leq a < b < c < 1 < d$. In this case the particle oscillates between b and c which is the only physical trajectory. This is because we require that both $0 \leq y(t) \leq 1$ and $U(y) \leq 0$. The case of three roots, when $b = c$, yields a constant trajectory in time which corresponds to the homogenous solution, $\rho_C(x) = y(2\beta x) = r_C$. The case where there are only two real roots does not correspond to any physical solution. The manifold which defines the region of $\{K, Q_A, Q_C\}$ -space where the physical solution resides is thus obtained by inserting the homogenous solution, $\rho_\alpha(x) = r_\alpha$, into (12) and (14) as

$$Q_{\alpha,h} = r_\alpha(r_{\alpha+2} - r_{\alpha+1}), \quad K_h = r_A r_B r_C + Q_A r_C - Q_C r_A. \quad (19)$$

The trajectory of (17) between b and c for $b < c$ yields the ordered profile of the ABC model corresponding to given values of K, Q_A and Q_C . In order to relate these parameters to the original parameters of the problem, β and r_α , we examine the period of oscillation of the particle between b and c , which we denote as Θ . The periodic boundary condition of the profile, $\rho_C(x+1) = \rho_C(x)$, imposes a constraint on the solution of the form, $y_m(t+2\beta) = y_m(t)$ or equivalently $\Theta = 2\beta/m$. Here, the positive integer parameter m corresponds to the number of times the particle oscillates between b and c in a time interval of length 2β . We argue in the next section that only the

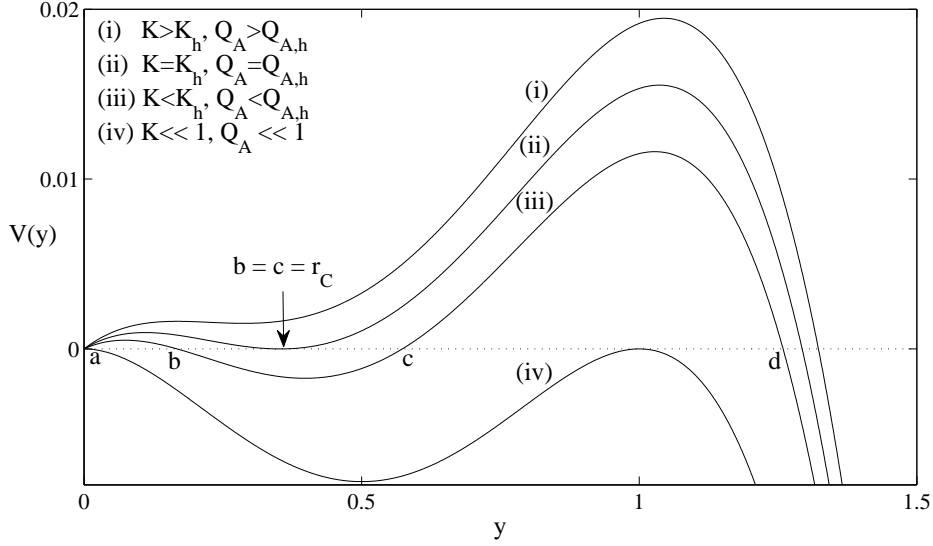


Figure 2. The effective potential, $U(y)$, for $r_A = r_B \neq r_C$ and some values of K, Q_A ($Q_C = 0$). (i), (ii) and (iii) represent the case where potential has 2,3 and 4 real roots. They correspond to the case of the model has no physical solution, a homogenous solution and an ordered solution, respectively. The four roots of the potential in (iii) are denoted on the graph by $\{a, b, c, d\}$. (iv) depicts the limit of $K \ll 1, Q \ll 1$ which corresponds to the low temperature limit ($\beta \gg 1$).

$m = 1$ solution describes the ordered steady state of the model. The periodic boundary condition may be written as

$$1 = \int_0^1 dx = \int_0^{2\beta} \frac{dt}{2\beta} = \frac{m}{\beta} \int_b^c \frac{dy}{\sqrt{-2U_{K,Q_A,Q_C}(y)}}. \quad (20)$$

An additional constraint on $y_m(t)$ comes from the total number of C particles,

$$r_C = \int_0^1 dx \rho_C(x) = \int_0^{2\beta} \frac{dt}{2\beta} y_m(t) = \frac{m}{\beta} \int_b^c \frac{y dy}{\sqrt{-2U_{K,Q_A,Q_C}(y)}}. \quad (21)$$

The third constraint is obtained by dividing (12) by ρ_α and integrating the result over x using periodic boundary conditions. For $\alpha = C$ the result yields the condition

$$\frac{r_B - r_A}{Q_C} = \int_0^1 dx \rho_C^{-1}(x) = \int_0^{2\beta} \frac{dt}{2\beta} y_m^{-1}(t) = \frac{m}{\beta} \int_b^c \frac{y^{-1} dy}{\sqrt{-2U_{K,Q_A,Q_C}(y)}}, \quad (22)$$

which is related to the difference between r_A and r_B and the consequent current of C particles. In Appendix A we provide an analytic expression for (20)-(22) using elliptic integrals.

In the following section we will analyze the phase diagram which arises from the solution above. For simplicity we restrict ourselves to the two nonequal densities case, $r_A = r_B \neq r_C$, which yields the same qualitative behaviour as the more general three nonequal densities case. For $r_A = r_B \neq r_C$ we find that $Q_C = J_C/\beta = 0$. This simplifies the form of the effective potential (18) and leaves us with only two constraints, (20) and

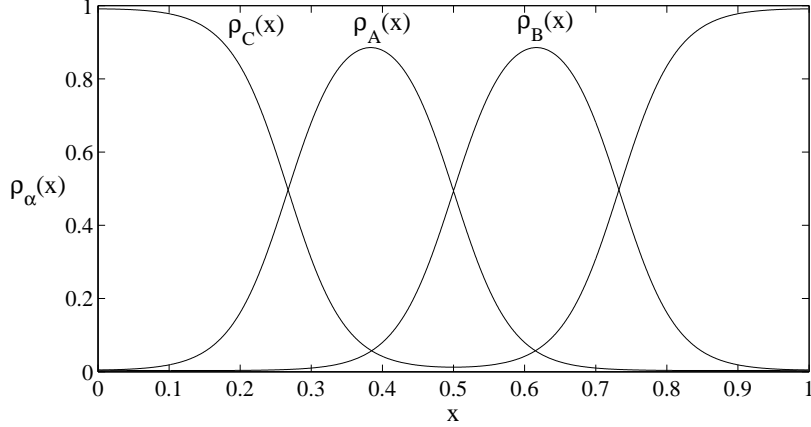


Figure 3. The ordered density profile obtained from (25) and (15) for $r_A = r_B \neq r_C$ with $\Delta = 0.1$, $\beta = 25$ and $m = 1$.

(21), which take the form of

$$\Theta = 2\beta/m = 2\kappa K(1/k)/k, \quad (23)$$

$$r_C = \frac{1}{3} + 2\Delta = \frac{1}{\alpha_-} \left[2 \frac{1 + \alpha_-/\alpha_+}{\beta k/m\kappa} \Pi(\alpha_-^2/\alpha_+^2 k^2, 1/k) - 1 \right]. \quad (24)$$

Here α_{\pm} , κ and k are functions of K, Q_A given in Appendix A and $K(k), \Pi(n, k)$ denote the complete elliptic integral of the first and third kind, respectively, whose definition is found in Appendix A as well. The profile of the C particles is expressed by inverting the equation $x = \int_0^t dt' = \frac{1}{2\beta} \int_b^y \frac{dy'}{\sqrt{-2U(y')}}$ as

$$\rho_C(x) = \frac{1 + \text{sn}(2\beta x/\kappa, k)}{\alpha_+ - \alpha_- \text{sn}(2\beta x/\kappa, k)}. \quad (25)$$

where sn is the Jacobi's elliptic function [22]. The dependence of the profile on m is hidden in the value of K, Q_A which set k, κ, α_{\pm} . The resulting $m = 1$ profile for a specific value of β is shown in figure 3. In the section below we study the behaviour of this solution and the resulting phase diagram. We also examine its behaviour at low temperature ($1 \ll \beta \ll L$) in Appendix B and find that it conforms with our physical understanding of the model.

It is interesting to note that the hydrodynamic equations of the ABC model (6) can be solved by considering a moving steady-state solutions of the form $\rho_{\alpha}(x, \tau) = \tilde{\rho}_{\alpha}(x + v\tau)$. However, such solutions did not appear in the numerical relaxation of (6) as well as in Monte Carlo simulations. This may mean, although remains to be proven, that moving solutions are unstable stationary solutions of the ABC dynamics. We therefore restricted our derivation to case of $v = 0$.

4. Phase diagram for nonequal densities

In this section we examine the behaviour of K, Q_A as we change the values of β and r_{α} for the two nonequal densities case. Their values are obtained by inverting the integral

conditions given in (20)-(21), which are written in an explicit form in (23)-(24).

For all values of β the hydrodynamic equations (6) have a stationary solution of the form $\rho_\alpha(x) = r_\alpha$, which corresponds to the homogenous values of $K = K_h$ and $Q_\alpha = Q_{h,\alpha}$ given in (19). As discussed in section 2, this solution becomes unstable below the critical line, $\beta > \beta_c = 2\pi\sqrt{3}/\sqrt{1 - 36\Delta^2}$. In this regime we expect to find an ordered solution. Figure 4 displays $T = 1/\beta$ computed according to (23) where Q_A is set for a given value of K through (24). For a small values of Δ , in figure 4a, we find a second order transition at $T = 1/\beta_c$ between the homogenous phase and the $m = 1$ ordered phase where $K < K_h$. This behaviour persists up to the tricritical point (9), which in the two nonequal densities case takes the simpler form of $\Delta = 1/(3 + 3\sqrt{3}) \simeq 0.122$. In figure 4b, we see that beyond the tricritical point, the $m = 1$ ordered phase appears also at $T > 1/\beta_c$. This is because the relation between K and β under a fixed value of Δ is non-monotonic. As a result the model is expected to undergo a first order transition between the two phases at value of β between the two stability limits. The discontinuity in K at the transition implies that this is a transition from a homogenous state to an ordered state with a finite amplitude of modulation.

In order to compute the first order transition point one has to know the full large deviation function (LDF) of the ABC model, which is not known. We may still draw the stability limits of the two phases defined by the critical temperature and the minimum of $K(\beta)$ in the ordered phase. The resulting stability lines are shown in figure 1 for the case of two nonequal densities.

In figure 5 we examine the first order transition using Monte Carlo simulations. The algorithm for the simulation is straightforward. At each step a site is selected at random and an exchange step is attempted where the particle in the chosen site may be exchanged with its neighbour to the right with probability given by (1). We measured the parameter $\langle \rho_A \rho_B \rho_C \rangle$ and compared it to that obtained from the hydrodynamic solution by integrating (14) over x . In the simulation it was measured by counting the number of ABC triplets in the lattice after each L exchange attempts and averaging the result over many such time steps.

In figure 5 we plot the simulation results for different values of temperatures around the first order transition and for various system lengths. For each value of T the simulation is initiated in the fully ordered phase and run for a time period which was sufficient to observe transitions between the two phases. The number of ABC triplets is averaged over the entire second half of the simulation where the system is unaffected by its initial state. The figure displays a first order phase transition, smoothen by finite size effects. The transition occurs below the critical point as suggested by our analysis. Near the transition point we observe slow fluctuations of the system between the two phases, as depicted in figure 6. This implies that the figure 5 might contain some errors near the transition point due to insufficient sampling time. We do not expect the transition point in the $L \rightarrow \infty$ limit to obey Maxwell's construction since the horizontal axis is not the conjugate variable of T . The latter can only be derived from full LDF of the model. Figure 5 also displays a good agreement with the theoretical

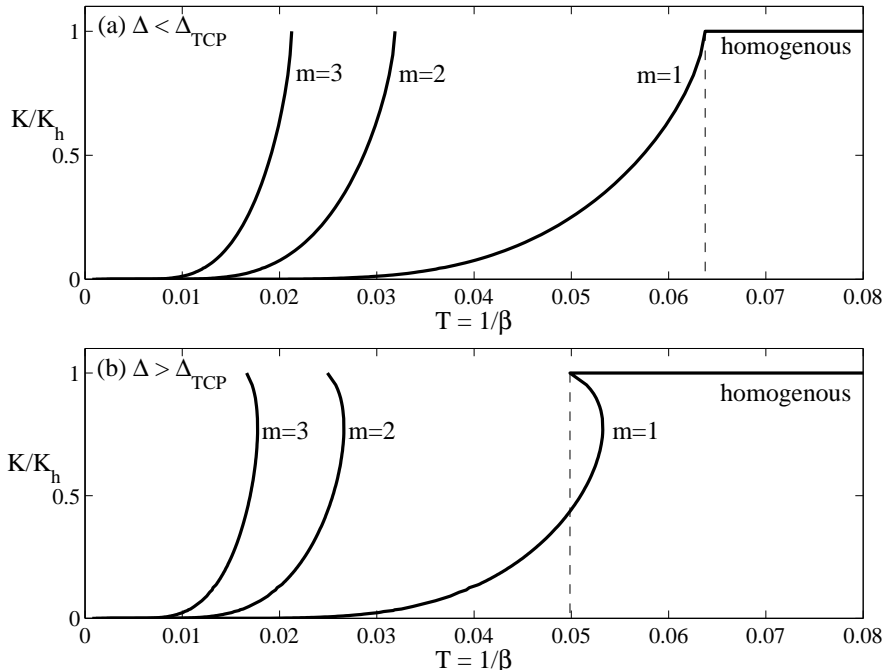


Figure 4. The temperature, $T \equiv 1/\beta = 2/m\Theta(K, Q_A)$, computed as a function of K for $m = 1, 2, 3$ for two nonequal densities, $r_A = r_B \neq r_C$. $Q_A(K, \Delta)$ is set by (24). The dashed line denotes the critical point $\beta = 2\pi\sqrt{3}/\sqrt{1 - 36\Delta^2}$. (a) and (b) are calculated for $\Delta = 0.12$ and $\Delta = 0.14$, respectively, depicting the case where Δ is below and above the tricritical point.

values for $\langle \rho_A \rho_B \rho_C \rangle$ above and below the transition point, which confirms the validity of the mean-field approximation (5).

Figure 6 depicts the fluctuations of the system between the ordered and disordered phases for $L = 4800$ at a temperature close the first order transition point. The figure shows significant and long-lived fluctuations around the ordered phase. A thorough investigation of their nature showed that they are not related to any known meta-stable state of the model and that they decay as the size of the system is increased. We avoid, however, using larger systems since they would require much longer simulation time to display transitions between the two phases.

In figure 4 we find that for $1/2\beta_c < T < 1/\beta_c$ the $m = 1$ is the only stable solution, whereas the $m > 1$ profiles are unstable. At lower temperatures the latter become stationary states and may theoretically be the ground state of the model. In the equal-densities case, this possibility has been ruled out by showing that the $m = 1$ profile has the lowest free energy for all $T < T_c$ [17]. For nonequal densities, a similar analysis would require the knowledge of the full LDF of the ABC model. Here, however, the fact that the $m = 1$ is the ground state of the model can be argued by noting that the m^{th} solution corresponds to an ordered state with particles segregated into $3m$ domains. Since lower temperatures (stronger drive) favour segregation, it is natural to assume that the most segregated state, $m = 1$, remains stable for $T < 1/2\beta_c$. We therefore

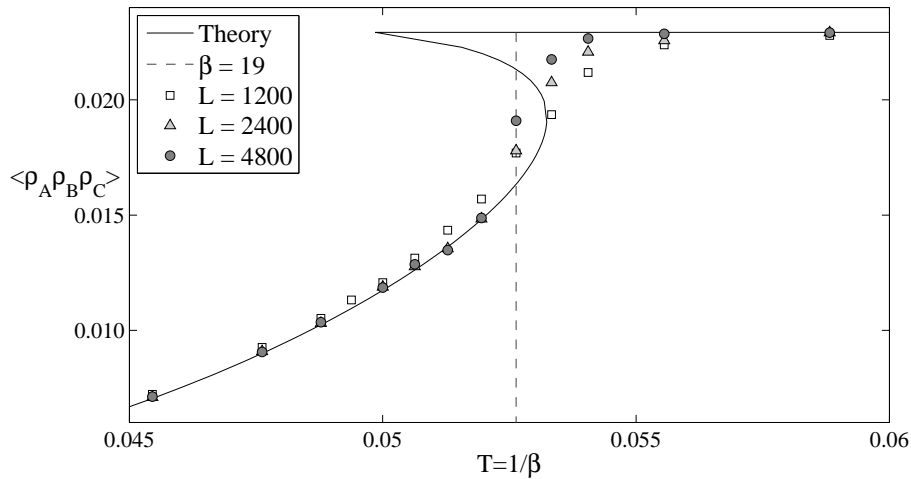


Figure 5. The density of ABC triplets as measured in simulation as a function of $T \equiv 1/\beta$ in comparison with the theoretical values (solid line). The simulation was performed for the two nonequal densities case with $\Delta = 0.14 > \Delta_{TCP} \simeq 0.122$ and various values of L . The dashed line denotes the value of $\beta = 19$ for which the time evolution of $\langle \rho_A \rho_B \rho_C \rangle$ is plotted in figure 6.

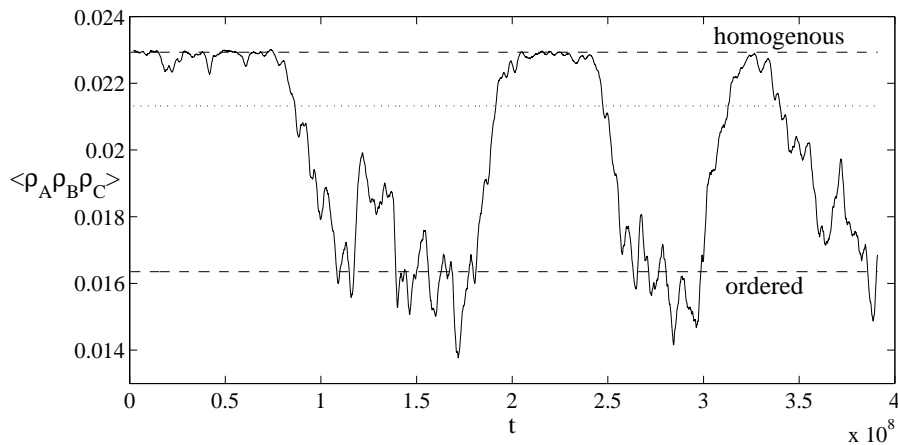


Figure 6. The density of ABC triplets as a function of time given by the number of Monte Carlo sweeps for $L = 4800$, $\Delta = 0.14$ and $\beta = 19$. The upper and lower dashed lines denote the theoretical values of the homogenous and ordered phases, respectively. The dotted line denotes the unstable ordered solution which, as expected, does not appear in the simulation.

consider it to be the steady-state solution of the model throughout the ordered phase. This argument is supported by Monte Carlo simulations of the model, where only the $m = 1$ profile was observed below the transition point.

5. Conclusions

In this paper we have derived an exact expression for steady-state density profile of the ABC model on a ring. The derivation is based on a hydrodynamic description of the model which has been suggested to be exact in the thermodynamic limit [17]. The solution is valid for the case where the average densities of each species are not equal and the model is thus out of equilibrium. Using this solution we have studied the first order phase transition whose existence was suggested by Clincy et al. The transition is of first order since there is a finite range of temperatures where the model has two stable phases. The transition point is located where the large deviation function of the two phases is equal. However, since this function has not yet been found we can only draw the stability limits of the two phases which define the coexistence region. Monte Carlo simulation of a specific point in parameter space confirmed that the first ordered phase transition occurs within the coexistence region, above the previously known critical temperature. The simulations also yielded a good agreement with the hydrodynamic solution in regions where only one phase is stable.

The present study opens the door for future studies of the ordered phase in the ABC model with arbitrary values of average densities. We plan to employ the solution obtained here in order to study the inequivalence of ensembles in the nonconserving ABC model with nonequal densities [15] and compare the results with those previously obtained for the equal-densities case [13, 14].

Acknowledgments

We thank Amir Bar, Martin R. Evans and Ori Hirschberg for helpful discussions. The support of the Israel Science Foundation (ISF) is gratefully acknowledged.

Appendix A. Analytic expression of the mean-field solution

In this appendix we obtain an analytic expression for the relation between the parameters of the effective potential K, Q_A, Q_C and the parameters of the model, β, r_α . We derive the explicit expression for the general case and then present its simpler form for the two nonequal densities case, $r_A = r_B \neq r_C$, mostly used in this study.

Appendix A.1. Three nonequal densities

In section 3 we mapped the mean-field dynamics of the ABC model to the motion of a particle in a quartic potential,

$$U_{K,Q_A,Q_C}(y) = -\frac{1}{8}y^2(1-y)^2 + \frac{2K + Q_C}{4}y - \frac{2Q_A + Q_C}{4}y^2 - \frac{Q_C^2}{8}. \quad (\text{A.1})$$

The parameters of the potential K, Q_A, Q_C are linked to the parameters of the model, β and r_α , through three conditions (20)-(22) which involve integration over the trajectory of the particle.

We begin with (20) which can be expressed in terms of the incomplete elliptic integral of the first kind defined here in the Jacobi form [22],

$$F(x, k) = \int_0^x \frac{dz}{\sqrt{(1-z^2)(1-k^2z^2)}}. \quad (\text{A.2})$$

Following a similar derivation as in [17] we introduce a Möbius transformation that maps the roots of the potential,

$$U_{K, Q_A, Q_C}(y) = 0 \quad \forall y \in \{a, b, c, d\}, \quad (\text{A.3})$$

onto the poles of the integrand in (A.2),

$$\{a, b, c, d\} \mapsto \{-1, -1/k, 1/k, 1\}. \quad (\text{A.4})$$

The transformation is given by

$$z = f(y) = \frac{d-a}{d+a} \frac{\alpha_+ y - 1}{\left(\alpha_- - \frac{2ad}{d+a} \alpha_+ \alpha_-\right) y + \left(1 + \frac{2ad}{d+a} \alpha_-\right)} \equiv \frac{Ay + B}{Cy + D}, \quad (\text{A.5})$$

where

$$\alpha_{\pm} = \frac{\pm(bc - ad) + \sqrt{(a-b)(a-c)(b-d)(c-d)}}{bc(a+d) - ad(b+c)}, \quad (\text{A.6})$$

and

$$k = \frac{1 + \alpha_- \left(b - a \frac{(b-c)(b-d)}{ab-2ad+cd}\right)}{1 - \alpha_+ \left(b - a \frac{(b-c)(b-d)}{ab-2ad+cd}\right)} \quad (\text{A.7})$$

The parameters $\alpha_-, \alpha_+, A, B, C, D$ and k are functions of K, Q_A, Q_C through a, b, c and d . Let $t(y)$ be the time it takes the particle to move from b to y . Using the transformation above it may be expressed as

$$\begin{aligned} t &= 2 \int_a^y \frac{dy'}{\sqrt{-2U(y')}} = \varkappa \int_{-1/k}^{f(y)} \frac{dz}{\sqrt{(1-z^2)(1-k^2z^2)}} \\ &= \varkappa [F(1/k, k) + F(f(y), k)], \end{aligned} \quad (\text{A.8})$$

where

$$\varkappa = \frac{2\sqrt{(C^2 - A^2)(C^2 - k^2A^2)}}{AD - BC} \quad (\text{A.9})$$

Equation (20), whereby the period of oscillation obeys $\Theta = 2\beta/m$, can be expressed by setting $f(y) = 1/k$ in (A.8). For that end we first notice that the integral in this equation can be brought to a simpler form in the new coordinates $w = kz$,

$$\begin{aligned} F(1/k, k) &= \int_0^{1/k} \frac{dz}{\sqrt{(1-z^2)(1-k^2z^2)}} \\ &= \int_0^1 \frac{dw/k}{\sqrt{(1-w^2/k^2)(1-w^2)}} = \frac{1}{k} K(1/k), \end{aligned} \quad (\text{A.10})$$

where $K(1/k)$ is the complete elliptic integral of the first kind. Using this form the condition of $\Theta = 2\beta/m$ can be written as

$$\frac{2m\kappa}{k}K(1/k) = \beta. \quad (\text{A.11})$$

The second condition (21) can be written in the form of

$$\begin{aligned} \frac{1}{2\beta} \int_0^{2\beta} y_m(t) dt &= \frac{m}{\beta} \int_b^c \frac{y dy}{\sqrt{-2U(y)}} = \\ \frac{m\kappa}{\beta} \int_{-\frac{1}{k}}^{\frac{1}{k}} \frac{-B + Dz}{A - Cz} \frac{dz}{\sqrt{(1-z^2)(1-k^2z^2)}} &= \\ \frac{m\kappa}{\beta} \int_0^{\frac{1}{k}} \frac{2}{AC} \left(\frac{AD - BC}{1 - \frac{C^2}{A^2}z^2} - DA \right) \frac{dz}{\sqrt{(1-z^2)(1-k^2z^2)}} &= \\ \frac{2m\kappa D}{\beta C} \left[\left(1 - \frac{BC}{AD} \right) \Pi \left(\frac{C^2}{A^2}, \frac{1}{k}, k \right) - F \left(\frac{1}{k}, k \right) \right]. \end{aligned} \quad (\text{A.12})$$

Here $\Pi(n, x, m)$ is the incomplete elliptic integral of the third kind [22] defined as

$$\Pi(n, x, k) = \int_0^x \frac{dz}{(1-nz^2)\sqrt{(1-z^2)(1-k^2z^2)}}. \quad (\text{A.13})$$

The third integral condition (22) is given by replacing A with B and C with D in (A.12),

$$\begin{aligned} \frac{1}{2\beta} \int_0^{2\beta} y_m^{-1}(t) dt &= \frac{m}{\beta} \int_b^c \frac{y^{-1} dy}{\sqrt{-2U(y)}} = \\ \frac{m\kappa}{\beta} \int_{-\frac{1}{k}}^{\frac{1}{k}} \frac{-A + Cz}{B - Dz} \frac{dz}{\sqrt{(1-z^2)(1-k^2z^2)}} &= \\ \frac{2m\kappa C}{\beta D} \left[\left(1 - \frac{AD}{BC} \right) \Pi \left(\frac{D^2}{B^2}, \frac{1}{k}, k \right) - F \left(\frac{1}{k}, k \right) \right]. \end{aligned} \quad (\text{A.14})$$

As in (A.10), these results can be written in terms of a complete elliptic integral using the transformation $w = kz$,

$$\begin{aligned} \Pi(n, 1/k, k) &= \int_0^{1/k} \frac{dz}{(1-nz^2)\sqrt{(1-z^2)(1-k^2z^2)}} \\ &= \int_0^1 \frac{dw/k}{(1-\frac{nw^2}{k^2})\sqrt{(1-\frac{w^2}{k^2})(1-w^2)}} = \frac{1}{k} \Pi\left(\frac{n}{k^2}, \frac{1}{k}\right). \end{aligned} \quad (\text{A.15})$$

Here $\Pi(n, k)$ is the complete elliptic integral of the third kind. The two integral conditions (21), (22) are thus given by

$$\frac{D}{C} \left[2 \frac{1 - BC/AD}{\beta k/m\kappa} \Pi \left(\frac{C^2}{k^2 A^2}, \frac{1}{k} \right) - 1 \right] = r_C, \quad (\text{A.16})$$

$$\frac{C}{D} \left[2 \frac{1 - AD/BC}{\beta k/m\kappa} \Pi \left(\frac{D^2}{k^2 B^2}, \frac{1}{k} \right) - 1 \right] = \frac{r_B - r_A}{Q_C}. \quad (\text{A.17})$$

In order to obtain $K(\beta, r_\alpha)$, $Q_A(\beta, r_\alpha)$ and $Q_C(\beta, r_\alpha)$ one has to invert (A.11), (A.16) and (A.17). Once this is done the profile can be computed by inverting (A.8). The result may be expressed using the Jacobi elliptic function, $\text{sn}(x, k)$, defined by the equation $F(\text{sn}(x, k), k) = x$. The profile of C particles is then given up to translations of x by

$$\rho_C(x) = \frac{-B + D \text{sn}(2\beta x / \varkappa, k)}{A - C \text{sn}(2\beta x / \varkappa, k)}. \quad (\text{A.18})$$

Note that the dependence on m is hidden in k, \varkappa, α_\pm . The two other profiles, $\rho_A(x)$ and $\rho_B(x)$, are obtained from (15) and $\rho_A(x) + \rho_B(x) = 1 - \rho_C(x)$.

Appendix A.2. Two nonequal densities

For convenience we write explicitly the solution for the two nonequal densities case, which is studied extensively in this paper. The form of the solution in this case is very similar to that obtained for equal densities in [17].

When $r_A = r_B \neq r_C$ it is easy to see from symmetry that $Q_C = J_C/\beta = 0$. As a result, our solution depends only on two parameters K, Q_A which are set by β, Δ . The latter is defined by

$$r_A = r_B = 1/3 - \Delta, \quad r_C = 1/3 + 2\Delta. \quad (\text{A.19})$$

The effective quartic potential which governs the motion of the particle is of the form

$$U_{K, Q_A, 0}(y) = -\frac{1}{8}y^2(1-y)^2 + \frac{K}{2}y - \frac{Q_A}{2}y^2 \quad (\text{A.20})$$

and its four roots are thus $\{0, b, c, d\}$. The Möbius transformation from these roots to the poles of the elliptic integral are obtained by setting $a = 0$ in the form presented in the previous section. More explicitly it is given by

$$z = f(y) = \frac{\alpha_+ y - 1}{\alpha_- y + 1}, \quad (\text{A.21})$$

where

$$\alpha_\pm = \frac{\pm bc + \sqrt{bc(d-c)(d-b)}}{bcd}, \quad (\text{A.22})$$

and

$$k = \frac{1 + \alpha_- b}{1 - \alpha_+ b}. \quad (\text{A.23})$$

Note that this form is identical to the one defined in the equal densities case [17].

We now express using elliptic integrals the two conditions that determine mapping between K, Q_A and β, Δ . The first condition is identical to (A.11),

$$2m\varkappa K(1/k)/k = \beta. \quad (\text{A.24})$$

where here \varkappa takes the simpler form of

$$\varkappa = \frac{2(\alpha_+ + \alpha_-)}{\sqrt{(1 - \alpha_+ b)(1 - \alpha_+ c)(1 - \alpha_+ d)}}. \quad (\text{A.25})$$

The second condition (21) is given in this case as

$$\frac{1}{\alpha_-} \left[2 \frac{1 + \alpha_-/\alpha_+}{\beta k / \varkappa m} \Pi \left(\frac{\alpha_-^2}{\alpha_+^2 k^2}, \frac{1}{k} \right) - 1 \right] = r_C = \frac{1}{3} + 2\Delta. \quad (\text{A.26})$$

The functions $K(\beta, \Delta)$, $Q_A(\beta, \Delta)$ are obtained by inverting (A.24) and (A.26). As in the previous section, we use the result to express the profile of the C particles,

$$\rho_C(x) = \frac{1 + \text{sn}(2\beta x / \varkappa, k)}{\alpha_+ - \alpha_- \text{sn}(2\beta x / \varkappa, k)}. \quad (\text{A.27})$$

The two other profiles, $\rho_A(x)$ and $\rho_B(x)$, are again obtained from (15) and $\rho_A(x) + \rho_B(x) = 1 - \rho_C(x)$.

Appendix B. Asymptotic behaviour at low temperatures

In this section we study the behaviour of the hydrodynamic solution of model at low temperature ($L \rightarrow \infty$, $1 \ll \beta \ll L$) for the case of two nonequal densities, $r_A = r_B \neq r_C$. This form will be especially useful in future studies of a generalized ABC model with nonconserving dynamics [15]. The $T = 0$ limit corresponds to $K = Q_A = 0$. Inserting this into (A.22), (A.23) and (A.25) we obtain

$$k = 1, \quad \alpha_{\pm} = 1, \quad \varkappa = 4. \quad (\text{B.1})$$

For $k = 1$ the elliptic integral in (A.24) diverges, corresponding to the limit of $\beta \rightarrow \infty$. The elliptic integral in (A.26) diverges as well, maintaining a finite value of r_C .

To study the low temperatures behaviour we assume that $K(\beta, \Delta)$ and $Q_A(\beta, \Delta)$ vanish for exponentially to leading order as

$$K \sim e^{-\beta\gamma_1}, \quad Q_A \sim e^{-\beta\gamma_2}. \quad (\text{B.2})$$

In order to find the coefficients γ_1 and γ_2 we first examine the behaviour of (A.24).

Here we analyze only the behaviour of the $m = 1$ solution, which is considered to be the ground state of the model (see section 4). We expand \varkappa and k around their value at $T = 0$ as

$$\varkappa = 4 + \varkappa_1(K, Q_A) \quad k = 1 + k_1(K, Q_A) \quad (\text{B.3})$$

where \varkappa_1 and k_1 are functions whose form is not written explicitly in order to avoid lengthy expressions. They obey $0 < \varkappa_1 \ll 1$ and $0 < k_1 \ll 1$. Expanding (A.24) to leading order in these functions [23] we find that

$$\ln(k_1) = -\beta/4 + O(1) \quad (\text{B.4})$$

The condition coming from the average density (A.26) involves an additional function,

$$\alpha_-/\alpha_+ = 1 - a_1(K, Q_A) \quad (\text{B.5})$$

which can be shown to obey $k_1 \ll a_1 \ll 1$. Expanding (A.26) in a_1 and k_1 to leading order [23] we obtain that

$$\ln(k_1) - 3 \ln(a_1) = 12\Delta \ln(a_1) + O(1). \quad (\text{B.6})$$

Solving (B.4) and (B.6) to lowest order in K and Q_A yields

$$K \sim e^{-\beta(1/3-\Delta)}, \quad Q_A \sim \begin{cases} e^{-\beta(1/3-\Delta)} & \Delta \geq 0 \\ e^{-\beta(1/3+2\Delta)} & \Delta < 0 \end{cases}, \quad (\text{B.7})$$

which agrees with form of $K \sim e^{-\beta/3}$ found in the equal densities case [19].

In order to interpret this result we observe the behaviour of (14) whereby

$$\rho_A(x)\rho_B(x)\rho_C(x) = K - Q_A\rho_C(x), \quad (\text{B.8})$$

and hence

$$\int_0^1 dx \rho_A(x)\rho_B(x)\rho_C(x) \sim e^{-\beta \min(\frac{1}{3}-\Delta, \frac{1}{3}+2\Delta)} = q^{\min(N_A, N_B, N_C)}. \quad (\text{B.9})$$

In the limit of $\beta \rightarrow \infty$ the number of triplets of ABC is governed by the probability of an event where in the fully separated state two particles of different species meet in the domain of the third species. This probability scales as $q^{\min(N_A, N_B, N_C)}$, because this event occurs with the highest probability in the smallest domain.

References

- [1] H Spohn. Long range correlations for stochastic lattice gases in a non-equilibrium steady state. *J. Phys. A*, 16:4275–4291, 1983.
- [2] P L Garrido, J L Lebowitz, C Maes, and H Spohn. Long-range correlations for conservative dynamics. *Phys. Rev. A*, 42(4):1954–1968, 1990.
- [3] J R Dorfman, T R Kirkpatrick, and J V Sengers. Generic long-range correlations in molecular fluids. *Annu. Rev. Phys. Chem.*, 45(1):213–239, 1994.
- [4] J M Ortiz de Zárate and J V Sengers. On the physical origin of long-ranged fluctuations in fluids in thermal nonequilibrium states. *J. Stat. Phys.*, 115:1341–1359, 2004.
- [5] T Sadhu, S N Majumdar, and D Mukamel. Long-range steady state density profiles induced by localized drive. *ArXiv e-prints*, arXiv:1106.1838, 2011.
- [6] M R Evans, D P Foster, C Godrèche, and D Mukamel. Spontaneous symmetry breaking in a one dimensional driven diffusive system. *Phys. Rev. Lett.*, 74(2):208–211, 1995.
- [7] R Lahiri and S Ramaswamy. Are steadily moving crystals unstable? *Phys. Rev. Lett.*, 79(6):1150–1153, 1997.
- [8] R Lahiri, M Barma, and S Ramaswamy. Strong phase separation in a model of sedimenting lattices. *Phys. Rev. E*, 61(2):1648–1658, 2000.
- [9] M R Evans, Y Kafri, H M Koduvely, and D Mukamel. Phase separation in one-dimensional driven diffusive systems. *Phys. Rev. Lett.*, 80(3):425–429, 1998.
- [10] M R Evans, Y Kafri, H M Koduvely, and D Mukamel. Phase separation and coarsening in one-dimensional driven diffusive systems: Local dynamics leading to long-range hamiltonians. *Phys. Rev. E*, 58:2764–2778, 1998.

- [11] M Clincy, B Derrida, and M R Evans. Phase transition in the abc model. *Phys. Rev. E*, 67:066115, 2003.
- [12] T Bodineau, B Derrida, V Lecomte, and F van Wijland. Long range correlations and phase transitions in non-equilibrium diffusive systems. *J. Stat. Phys.*, 133:1013–1031, 2008.
- [13] A Lederhändler and D Mukamel. Long-range correlations and ensemble inequivalence in a generalized abc model. *Phys. Rev. Lett.*, 105(15):150602, 2010.
- [14] A Lederhändler, O Cohen, and D Mukamel. Phase diagram of the abc model with nonconserving processes. *J. Stat. Mech: Theory Exp.*, 2010(11):P11016, 2010.
- [15] O Cohen and D Mukamel. to be published.
- [16] M Kac, G E Uhlenbeck, and P C Hemmer. On the van der waals theory of the vapor-liquid equilibrium. *J. Math. Phys.*, 4(2):216–228, 1963.
- [17] A Ayyer, E A Carlen, J L Lebowitz, P K Mohanty, D Mukamel, and E R Speer. Phase diagram of the abc model on an interval. *J. Stat. Phys.*, 137(5-6):1166–1204, 2009.
- [18] J Barton, J L Lebowitz, and E R Speer. The grand canonical abc model: a reflection asymmetric mean-field potts model. *J. Phys. A*, 44(6):065005, 2011.
- [19] J Barton, J L Lebowitz, and E R Speer. Phase diagram of a generalized abc model on the interval. *ArXiv e-prints*, arXiv:1106.1942, 2011.
- [20] M R Evans. Phase transitions in one-dimensional nonequilibrium systems. *Braz. J. Phys.*, 30:42–57, 2000.
- [21] G Fayolle and C Furtlehner. Stochastic deformations of sample paths of random walks and exclusion models. In M Drmota, P Flajolet, D Gardy, and B Gittenberger, editors, *Mathematics and Computer Science III: Algorithms, Trees, Combinatorics and Probabilities (Trends in Mathematics)*, pages 415–427. Birkhäuser, Basel, 2004.
- [22] M Abramowitz and I Stegun. *Handbook of Mathematical Functions with Formulas, Graphs and Mathematical Tables*. National Bureau of Standards Appl. Math. Series, 1964.
- [23] Inc. Wolfram Research. *Mathematica Edition: Version 8.0*. Wolfram Research, Inc., Champaign, Illinois, 2010.